

# UC Santa Barbara

## UC Santa Barbara Previously Published Works

### Title

Stochastic modeling of climatic variability in dendrochronology

### Permalink

<https://escholarship.org/uc/item/47r2h953>

### Journal

Geophysical Research Letters, 31(15)

### ISSN

0094-8276

### Authors

Lavallée, Daniel

Beltrami, Hugo

### Publication Date

2004-08-01

Peer reviewed

## Stochastic modeling of climatic variability in dendrochronology.

Daniel Lavallée<sup>1\*</sup> and Hugo Beltrami<sup>2</sup>

1 Institute for Crustal Studies, University of California, Santa Barbara. \* corresponding author

2 Environmental Earth Sciences Laboratory, St. Francis Xavier University, Antigonish, Nova Scotia, Canada.

**Abstract:** Climatic variability can be characterized by invariant quantities arising from the analysis of scaling properties of paleoclimatic records. In this paper we discuss a stochastic model that reproduces the variability and the long-range correlation observed in dendrochronological time series. We have found that non-Gaussian distributions are better suited to describe the climatic variability embedded in these data. Our results indicate that Gaussian distribution fails to capture the large fluctuation —extreme events— that characterized climatic variability in these time series. This might have applications on the study of extreme weather events on future climate scenarios.

### 1. Introduction

Most records of climate change show increase warming since the industrial revolution [Houghton *et al.*, 2001]. Furthermore, it has also been shown that at the climate system scale, that oceans, cryosphere, atmosphere and continental areas have absorbed heat in the last 50 years on the order of 182.0, 8.1, 6.6 and 7.1 ( $10^{21}$ ) Joules respectively [Levitus, 2000; Beltrami *et al.*, 2002; Beltrami, 2002]. The question is whether the additional energy available in the climate system coupled to anthropogenic changes in the environmental conditions at the Earth's surface, for example, due to land use changes, might lead to a more vigorous atmospheric circulation and thus our climate might experience an increased number of extreme weather events. Such a change has serious implications for society and has attracted much attention from policy makers and the general public. In order to assess the number, magnitude, and character of extreme weather events in a future warmer climate, models of the climate system have been used to study

the statistics of climate model outputs [*e.g.* Hegerl *et al.*; 2003, Kharin and Zwiers, 2003]. To assess whether the frequency of extreme weather events will increase in a warmer future Earth's climate, it is also important to understand and model the frequency of occurrence of extreme weather events in the past. One of the records with highest resolution of past environmental conditions, in temperate latitudes, are dendrochronological data. Tree ring records have been routinely used to reconstruct past climatic changes [*e.g.* Cook and Briffa, 1990; Stahle *et al.*, 2000; Cook *et al.*, 2000; Esper *et al.*, 2001; 20002]. Recent multiproxy reconstructions of the past climate of the northern hemisphere made important use of dendrochronological records [*e.g.* Mann *et al.*, 1999, see chapter 2 in Houghton *et al.*, 2001].

In this letter, we examine four long dendrochronological records from the western United States selected from the International Tree Ring Databank (ITRDB) (see Table 1). The tree ring data were selected for this study because of their large temporal coverage and their likelihood to be moisture or temperature sensitive.

One important feature of the dendrochronological data is its complex behavior (see Figure 1). Note that the time evolution of the signal is erratic showing no apparent regularity or cyclic pattern. In this letter, we propose to decipher the “complexity” embedded in the dendrochronological records in term of its statistical properties. For this purpose, we present a stochastic model that reproduce the probability law and correlation function (or power spectrum) observed in the dendrochronological records.

## **2. Formulation of the stochastic model:**

To analyze the complex behavior of the dendrochronological time series, a typical procedure consists in performing a Fourier analysis of the time series. The power spectrum of one time series is illustrated in Figure 2. The spectrum shows that there are no dominating frequencies, and that these signals cannot be reduced to—or understood as— a combination of several

periodical functions. Figure 2, shows that all the frequencies contribute to the signals but also that the weight of the frequencies follows —on average— a trend given by a decaying power law. The values of the scaling exponents  $\nu$  are reported in Table 2.

The behavior reported in Figures 2 is typical of colored noises. According to this, a stochastic model can capture and reproduce some of the main features characterizing the dendrochronological time series. The stochastic model proposed here consists of a convolution in the frequency space between the Fourier transform of random variables (white noise)  $X$  and some function with a power law dependence  $\omega^{-\nu/2}$ . The scaling exponent  $\nu$  measures the departure from the non-correlated random variable (white noise with  $\nu=0$ );  $\omega$  is the angular frequency. This stochastic process is similar to a fractional Brownian motion that reduces to a random walk in its simplest manifestation —with  $\nu=2$  and  $X$  a Gaussian random variable [see Peitgen and Saupe, 1988; and Falconer, 1990]. In this study, the parameter  $\nu$  and the probability law that governs the distribution of the random variables are unspecified. They are determined through a statistical analysis of the data. The stochastic model  $Y_t$  is given by the following relationship:

$$Y_t \propto \sum_{s=1}^N \omega^{-\nu/2} F_\omega[X_t] \exp[2\pi i(t-1)(s-1)/N] , \quad (1)$$

for a set of random variables  $X_t$  distributed over a one-dimensional lattice of length  $N$ , where  $t$  is the integer time variable on the one-dimensional lattice. The sum in equation (1) goes from 1 to  $N$ ;  $s$  is related to  $\omega$  by  $\omega = 2\pi(s-1)$  and corresponds to a discrete frequency with integer values;  $F_\omega[X_t]$  is the discrete Fourier transform of the random variables. According to this, the power spectrum  $P(k)$  associated to  $Y_t$  will be given by the following relation:

$$P(\omega) = |F_\omega[Y_t]|^2 \propto \omega^{-\nu} . \quad (2)$$

This equation can be used to compute the values of the parameter  $\nu$  associated to  $Y_t$ . Using this scaling exponent  $\nu$ , the underlying random variables  $X_t$  associated to a stochastic model  $Y_t$  can be computed by using the following relationship:

$$X_t \propto F_t^{-1}[F_\omega[Y_t] \times \omega^{\nu/2}], \quad (3)$$

where  $F_t^{-1}$  is the Fourier inverse. The statistical properties of the stochastic model are completely specified when the probability law governing  $X_t$  are identified. The probability law controls the variability of the stochastic model while  $\nu$  constraints its long-range correlation [see *Lavallée and Archuleta, 2003* for another application of this stochastic model]

### 3. Stochastic model for dendrochronological time series:

In this letter, we assume that a dendrochronological time series can be approximated by a stochastic model  $Y_t$  described above. Using relation (2), the scaling exponent  $\nu$  of each time series has been computed. Then, using  $\nu$  and Eq. (3), the underlying random variables  $X_t$  associated to each time series are estimated. The number of random variables in the time series varies between 1666 (nv512) to 1967 (nv500). These numbers are large enough to perform the ensuing statistical analysis. For each tree ring sample, the probability density function (PDF) associated with  $X_t$  is thus estimated.

We then proceed to determine the probability law that will provide the best fit to the estimated PDF of  $X_t$ . Three candidates are considered: the Gauss law, the Cauchy law and the more general Lévy law [*Uchaikin and Zolotarev, 1999*]. The Lévy law is characterized by four parameters  $\alpha$ ,  $\beta$ ,  $\gamma$  and  $\mu$ . The parameter  $\alpha$ , with  $0 < \alpha \leq 2$ , controls the rate of falloff of the tails of the PDF. The larger the value of  $\alpha$ , the less likely it is to find a random variable far away from the central location. The case  $\alpha = 2$  corresponds to the Gaussian law while  $\alpha = 1$  (with  $\beta = 0$ ) corresponds to the Cauchy law. The parameter  $\beta$ , with  $-1 \leq \beta \leq 1$ , controls the departure

from symmetry of the PDF curve. When  $\beta = 0$ , the PDF is symmetric and centered about  $\mu$ . The parameter  $\gamma$ ,  $\gamma > 0$ , is mainly responsible for the PDF width whereas  $\mu$  is the location or shift parameter of the PDF.

For each tree ring sample, we have computed the probability law parameters that minimize the following expression:

$$\sum_t |PDF(X_t) - p_{th}(X_t)| \quad (4)$$

where  $p_{th}(X)$  corresponds the theoretical values of the PDF associated to either the Gauss, Cauchy or Lévy law computed for  $X$  [see *Grigoriu, 1995*]. The PDF of  $X$  and the PDF curves corresponding to the best-fitting Gaussian, Cauchy and Lévy law are illustrated in Figures 3, 4 and 5. For each tree ring sample, the parameters of the best-fitting Gaussian, Cauchy and Lévy laws are reported in Table 2. For each sample used in this study, the Lévy law provided the best fit to the PDF. For instance, the minimum values of the objective function given in Eq. (4) computed for the Cauchy, Gauss and Lévy laws are respectively: 0.0049, 0.0023 and 0.0013 for nv512. Note also that if we perform the same analysis over a comparable number of generated Cauchy, Gauss and Lévy random variables characterized by parameter values similar to those reported in Table 2, we will be able to recover the parameters values with enough accuracy to distinguish the three laws. In Figures 4 and 5, comparison of the tails of the PDF to the tail of the best fitting Gaussian and Cauchy curves confirms that the a Lévy law with  $1 < \alpha < 2$  provides a better fit.

Variation in the model parameters from one sample to another may suggest a spatial dependence. However, the variation may also reflect, at least partially, the presence of additional noisy effects and other uncertainties in the data. Further investigations are needed to reach a definitive conclusion.

For the four samples under studies, the value of the Lévy index  $\alpha$  doesn't vary very much from one sample to another. This suggests that the value of  $\alpha$  may be universal or independent of the tree location. Furthermore, the parameter  $\alpha$ , controls the decrease of the PDF tail. That is the occurrence of large fluctuations or extreme events in the data. For instance, using the parameters given in Table 2, one can easily compute, for a given period of time, the number of time that  $X$  that exceed a given threshold value. For dendrochronological data, these large fluctuations could be understood as abrupt climatic change. For the four samples, our results suggest that the probability to observe such events decreases almost at the same rate. The parameters  $\beta$  and  $\gamma$  reported in Table 2 indicate significant variation in the values estimated from one sample to another. (It should be noted that the values estimated for the parameter  $\gamma$  will depend on the definition adopted for the inverse Fourier transform used in Eq. (3). However, the values of  $\alpha$  and  $\beta$  are not affected by this definition.) Note that for  $s = 1$ ,  $\omega = 0$  in the convolution given by Eq. (3). This implies that the average value of the random variables estimated with Eq. (3) will be zero. This will affect the values taken by the location parameter  $\mu$  and suggest that not to much importance should be granted to the values taken by this parameter.

Finally note that the values taken by the parameters of the Levy law provide valuable information about the variability of the time series. The parameter  $\gamma$  controls the amplitude of the variability. This is why departures (or fluctuations) from the average trend of the time series are larger in Figure 1a than in Figure 1b as suggested by the estimated  $\gamma$  reported in Table 2. For a positive  $\beta$ , the tail of the PDF will decay more rapidly for negative values indicating that positive values are more likely to be observed. This implies for a time series approximated by a stochastic model given by Eq. (1) that positive jumps from the average values are more likely to be observed. The converse applies to negative value of  $\beta$  [see Figure 4.13 in *Uchaikin and Zolotarev, 1999*]. Although it is not necessary easy to capture on a plot the isolated effect due to

one parameter of the Lévy law when comparing two signal characterized by four different parameter values, comparison of Figures 1a to 1b illustrates well the consequences due to a variation in the polarity of the parameter  $\beta$ .

#### 4. Conclusion

In this paper, we investigated the variability of four dendrochronological records. We have shown that a stochastic model — based on Lévy law— is best suited to reproduces the main features of the climatic variability embedded in dendrochronological time series, including the presence of large fluctuations. (For a comparison between synthetic earthquake slips based on random variables distributed according to a Cauchy law and a Gauss law see Figure 4 in Lavallée and Archuleta 2003.) These results suggest some features of the complexity recorded in tree ring indices are quite general, perhaps “universal,” and thus can be formulated in term of the stochastic model discussed in this letter. Five parameters are needed to completely determine the stochastic model: the four parameters of the Lévy law controlling the amplitudes of the signal fluctuations and a scaling exponent to specify the correlation.

We already have indicated that the parameter  $\alpha$  controls the rate at which the probability to observe extreme events is decreasing. That is, for dendrochronological data, large climatic departure from the “usual” variability observed in the data. In principle the same procedure outlined in this letter can be applied to other paleoclimatic time series such as ice core data, stagalagmite data as well as to temperature time series recorded in recent years. Comparisons of the  $\alpha$  values computed for such time series, or for different period of times, will indicate the time dependence of the parameter  $\alpha$ , and therefore the time dependence in the rate at which the probability to observe abrupt climatic change is decreasing.

**Acknowledgements.** We appreciate the thoughtful comments of the reviewers, Dr. Bodri and Dr. Putnam, who have helped to clarify the contents of this paper. We also thank Dr. Jones for



his suggestions and his reading of the papers. Computations were performed using Mathematica 4.2 (Wolfram Research, Inc., 1999). The research reported in this paper was undertaken when the first author was appointed the W. F. James Professor of Pure and Applied Sciences at St. Francis Xavier University during the summer of 2003. This is ICS contribution No. 642.

## References

- Beltrami, H., Climate from borehole data: Energy fluxes and temperatures since 1500, *Geophys. Res. Lett.*, 29, (23), 2111, 10.1029/2002GL015702, 2002.
- Beltrami, H., J. Smerdon, H. N. Pollack and S. Huang, Continental heat gain in the global climate system, *Geophys. Res. Lett.*, 29, (8) 10.1029/2001GL014310, 2002.
- Chambers, J. M., C. L. Mallow, and B. W. Stuck. A Method for Simulating Stable Random Variables. *J. Amer. Stat. Assoc.*, 71, 304-344, 1976.
- Cook, E.R., Briffa, K.R. A comparison of some tree-ring standardization methods. In: E.R. Cook and L.A. Kairiukstis, eds., *Methods of Dendrochronology: Applications in the Environmental Sciences*. International Institute for Applied Systems Analysis, Kluwer Academic Publishers, Boston, MA: 153-162, 1990.
- Cook E.R., Buckley B.M., D'Arrigo R.D., and Peterson, M.J.. Warm-season temperatures since 1600 B.C. reconstructed from Tasmanian tree rings and their relationship to large-scale sea surface temperature anomalies. *Climate Dynamics* 16(2/3), 79-91, 2000
- Falconer, K. *Fractal geometry*. John Wiley & sons, Chichester. 288pp., 1990.
- Esper, J., Cook, E.R., Schweingruber, F.H. Low-frequency signals in long tree-ring chronologies for reconstructing past temperature variability. *Science* 295: 2250-2253, 2002.
- Esper, J., Treydte, K., Gärtner, H., Neuwirth, B. A tree ring reconstruction of climatic extreme years since 1427 AD for western central Asia. *Palaeobotanist* 50: 141-152, 2001.
- Grigoriu, M. *Applied Non-Gaussian Processes*. PTR Prentice Hall, Englewood cliffs, NJ. 442pp., 1995.
- Hegerl, G. C., F. Zwiers, S. Kharin and Peter Stott: Detectability of anthropogenic changes in temperature and precipitation extremes. *J. Climate*, *prov. accepted*.
- Houghton, J. T., G. J. Jenkins, and J. J. Ephraums (Ed.), *Climate change 2001 : the scientific basis : contribution of Working Group I to the third assessment report of the Intergovernmental Panel on Climate Change*. Edited by J.T. Houghton, Y. Ding, D.J. Griggs, M.Noguer, P.J. van der Linden, X. Dai, K. Maskell, and C.A. Johnson (eds), Cambridge University press, Cambridge, U.K. and New York, USA, 881 pp., 2001.
- ITRDB, Contributors of the International Tree-Ring Data Bank, IGBP PAGES/World Data Center for Paleoclimatology, NOAA/NGDC Paleoclimatology Program, Boulder, Colorado, USA.
- Kharin, V.V., and F.W. Zwiers. Estimating extremes in transient climate change simulations. Submitted to *Journal of Climate*, 2003.
- Lavallée, D. and R. J. Archuleta. Stochastic modeling of slip spatial complexities for the 1979 Imperial Valley, California, earthquake. *Geophys. Res. Lett.*, **30** (5), 1245, doi:10.1029/2002GL015839, 2003.
- Levitus, S., J. Antonov, J. Wang, T. L. Delworth, K. Dixon, and A. Broccoli, Anthropogenic warming of the Earth's climate system, *Science*, 292, 267-270, 2001.

- Mann, M. E., R. S. Bradley, and M. K. Hughes. Northern hemisphere temperatures during the past millennium: Inferences, uncertainties, and limitations, *Geophys. Res. Lett.*, 26,759-762, 1999.
- Nikias, C. L., and M. Shao. *Signal Processing with Alpha-Stable Distributions and Applications*. Jon Wiley & Sons, New York. 168pp. 1995.
- Paul, W., and J. Baschnagel. *Stochastic Processes From Physics to Finance*. Springer, Berlin. 231pp. 1999.
- Peitgen, H-O., and D. Saupe. *The Science of Fractal Images*. Springer-Verlag, New York. 312pp. 1988.
- Stahle, D.W., Cook, E.R., Cleaveland, M.K., Therrell, M.D., Meko, D.M., Grissino-Mayer, H.D., Watson, E. and Luckman, B.H. Tree-ring data document 16th century megadrought over North America. *EOS, Transactions of the American Geophysical Union* 81(12),121,125, 2000.
- Uchaikin, V. V., and V. M. Zolotarev. *Chance and Stability*. VSP, Utrecht, The Netherlands. 570pp, 1999.

D. Lavallée, Institute for Crustal Studies, University of California, Santa Barbara, CA93106 (email: [daniel@crustal.ucsb.edu](mailto:daniel@crustal.ucsb.edu)). Hugo Beltrami, Environmental Earth Sciences Laboratory, St. Francis Xavier University, Antigonish, Nova Scotia, Canada, B2G 2W5, (e-mail: [hugo@stfx.ca](mailto:hugo@stfx.ca).)

### Figure and table captions

**Figure 1:** The typical behavior of the time evolution of the tree ring indices is illustrated: (a) nv500 and (b) nv512. The time interval is one year on each sample.

**Figure 2:** For the signal illustrated in Figure 1a, the power spectrum  $P(\omega)$  has been computed. The power spectrum  $P(\omega)$  (red) and the best straight line (black) that fits the log-log curve is reported for this signal. These results suggest that the scaling behavior is observed for time scale length ranging from 2 to 512 years. The scaling exponent is given in Table 2.

**Figure 3:** The (discrete) probability density function PDF (red and blue dots and bars) associated to the filtered signal is illustrated: (a) nv500 and (b) nv512. The left side of the PDF ( $X < 0$ ) is colored in red while the right ( $X > 0$ ) side is in blue. The magnitude of the random variables is given by  $X$ . The width of the bar corresponds to the increment used to estimate the PDF is equaled to 50. The curves of three probability laws that best fit the PDF are illustrated: the

Cauchy law (black curve), the Gaussian law (dashed curve) and the Lévy law (green curve). The parameters of the Gaussian, Cauchy and Lévy law are reported in Table 2.

**Figure 4:** On a log-log plot, the left tail of the (discrete) probability density function PDF (red dot) associated to the filtered signal is illustrated for nv512. The curves of three probability law that best fit the PDF are illustrated: the Cauchy law (black curve), the Gaussian law (dashed curve) and the Lévy law (green curve). Tails that decay according to power laws characterized the Lévy and Cauchy probability density functions. Such behavior is best illustrated on a log-log plot. The misfit of the Gaussian probability density function is more obvious in these plots (see also Figure 5). In particular, note that according to the Gaussian law, the large events have almost a zero probability of being observed.

**Figure 5:** Same as for Figure 4, but for nv500 and for the right tail of the (discrete) PDF (blue dot).

**Table 1:** The dendrochronological data used in this study.

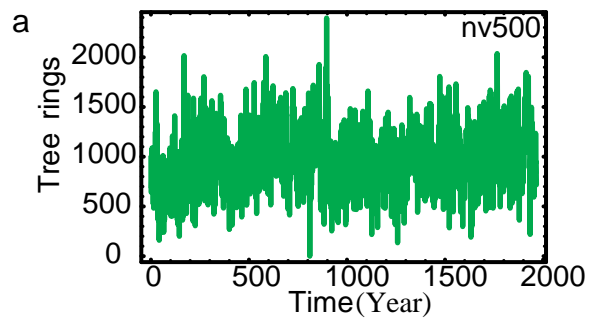
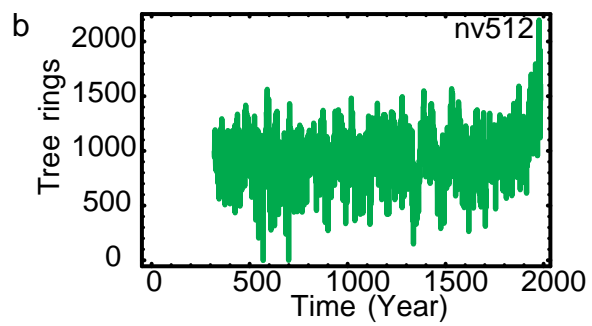
**Table 2:** Parameters of the stochastic models for the four tree ring indices: nv500, nv512, nv514 and ut508. The parameter  $\nu$  is the scaling exponent of the power spectrum (see Figure 2). The parameters of the Gauss law ( $\mu$  and  $\sigma$ ), the Cauchy law ( $\gamma$  and  $\mu$ ) and the Lévy law ( $\alpha$ ,  $\beta$ ,  $\gamma$  and  $\mu$ ) that best fit the four PDF( $X$ ) are given (see Figures 3, 4 and 5).

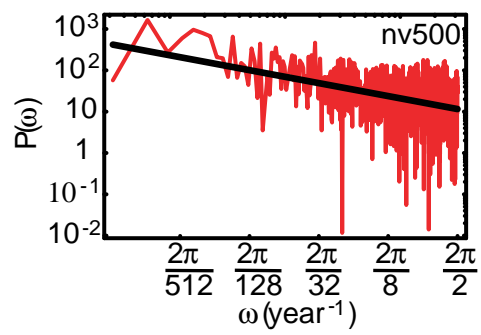
Table 1

Tree Ring	Location	Species	Years
nv500	38 <sup>0</sup> -57'N - 114 <sup>0</sup> -	Bristlecon Pine	1-1967
nv512	40 <sup>0</sup> -14'N- 115 <sup>0</sup> -	Bristlecon Pine	320-1985
nv514	40 <sup>0</sup> -33'N - 114 <sup>0</sup> -	Bristlecon Pine	302-1985
ut508	39 <sup>0</sup> -25'N-111 <sup>0</sup> -04'W	Bristlecon Pine	286-1985

Table 2

Samples	Scaling Exponent	Gauss law		Cauchy law		Lévy law			
		$\mu$	$\sigma$	$\gamma$	$\mu$	$\alpha$	$\beta$	$\gamma$	$\mu$
nv500	0.52	-3.59	153.	117.	-8.67	1.72	0.22	3211	9.99
nv512	0.63	15.23	99.1	76.8	16.43	1.62	-0.49	953	-5.73
nv514	0.7	-4.04	94.7	71.7	-6.42	1.76	0.28	1567	5.03
ut508	0.56	17.31	147.	110.	22.12	1.74	-1.0	3131	-21.1

**Figure 1a****Figure 1b**

**Figure 2**

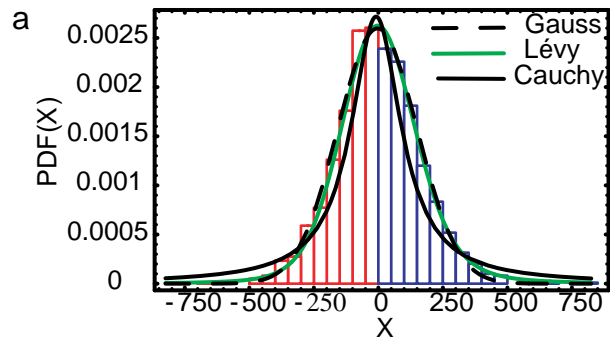


Figure 3a

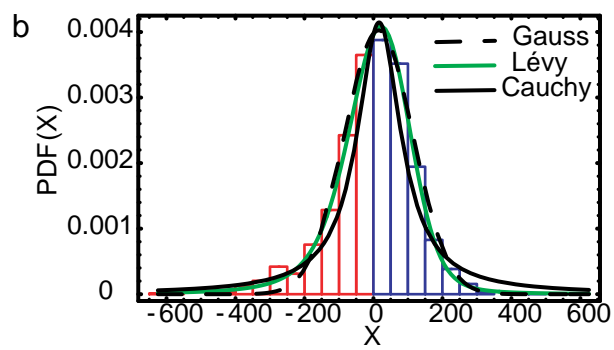
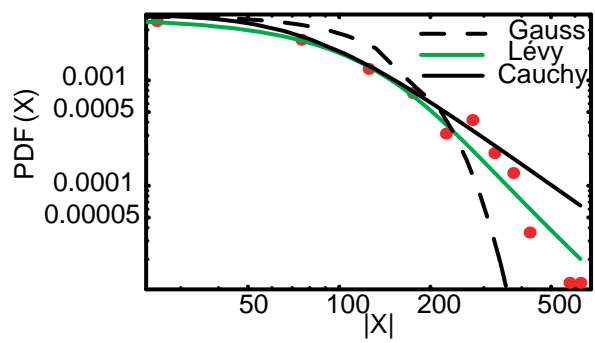
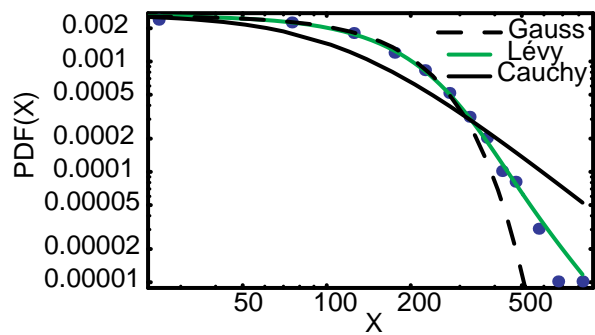


Figure 3b

**Figure 4**



**Figure 5**